# CD16xCD33 bispecific killer cell engager (BiKE) activates natural killer (NK) cells from myelodysplastic syndrome (MDS) patients against primary MDS and myeloid-derived suppressor cell (MDSC) CD33-positive targets

A THESIS SUBMITTED TO THE FACULTY OF THE GRADUATE SCHOOL OF THE UNIVERSITY OF MINNESOTA BY

Michelle K. Gleason, PhD

IN PARTIAL FULFILLMENT OF THE REQUIREMENTS
FOR THE DEGREE OF
MASTER OF SCIENCE

Advisor: Julie A. Ross, PhD, MPH

November 2014

**Acknowledgements**

Originally published by the American Society of Hematology in the journal *Blood*. Volume 123(196), Pages: 3016-3026.

Michelle K. Gleason (Department of Pediatrics, Division of Epidemiology and Clinical Research, University of Minnesota, Minneapolis, MN), Julie A. Ross (Department of Pediatrics, Division of Epidemiology and Clinical Research, University of Minnesota, Minneapolis, MN), Erica D. Warlick (Department of Medicine, Division of Hematology, Oncology, and Transplantation, University of Minnesota, Minneapolis, MN), Troy C. Lund (Department of Pediatrics, Division of Blood and Marrow Transplantation, University of Minnesota, Minneapolis, MN), Michael R. Verneris (Department of Pediatrics, Division of Blood and Marrow Transplantation, University of Minnesota, Minneapolis, MN), Andres Wiernik (Department of Medicine, Division of Hematology & Oncology, Hennepin County Medical Center, Minneapolis, MN), Stephen Spellman (Center for International Blood and Marrow Transplant Research (CIBMTR), National Marrow Donor Program (NMDP), Minneapolis, MN), Michael D. Haagenson (Center for International Blood and Marrow Transplant Research (CIBMTR), National Marrow Donor Program (NMDP), Minneapolis, MN), Alexander J. Lenvik (Department of Medicine, Division of Hematology, Oncology, and Transplantation, University of Minnesota, Minneapolis, MN), Mark R. Litzow (Department of Medicine, Division of Hematology, Mayo Clinic, Rochester, MN), Pearlie K. Epling-Burnette (Department of Hematologic Malignancies, H. Lee Moffitt Cancer Center and Research Institute, Tampa, FL), Bruce R. Blazar (Department of Pediatrics, Division of Blood and Marrow Transplantation, University of Minnesota, Minneapolis, MN), Louis M. Weiner (Department of Oncology, Lombardi Comprehensive Cancer Center, Georgetown University, Washington, DC), Daniel J. Weisdorf (Department of Medicine, Division of Hematology, Oncology, and Transplantation, University of Minnesota, Minneapolis, MN), Daniel A. Vallera (Department of Therapeutic Radiology-Radiation Oncology, University of Minnesota, Minneapolis, MN), Jeffrey S. Miller (Department of Medicine, Division of Hematology, Oncology, and Transplantation, University of Minnesota, Minneapolis, MN).



This work was supported in part by NIH P30 CA77598 utilizing the following Masonic Cancer Center, University of Minnesota shared resources: sample procurement and cell processing services from the Translational Therapy Core and Minnesota Masonic Charities through the Cancer Experimental Therapeutics Initiative (CETI). These studies were also supported in part by P01 CA111412, P30 CA77598, NIH T32 CA099936, K05 CA157439, R01 CA142714, the Minnesota Masonic Charities, the US Public Health Service Grants R01-CA36725, the Randy Shaver Foundation, the Lion's Children's Cancer Fund, the William Lawrence and Blanche Hughes Fund, and a grant from the

University of Minnesota-Mayo Clinic Partnership. The CIBMTR is supported by Public Health Service Grant/Cooperative Agreement U24-CA76518 from the National Cancer Institute (NCI), the National Heart, Lung and Blood Institute (NHLBI) and the National Institute of Allergy and Infectious Diseases (NIAID); a Grant/Cooperative Agreement 5U01HL069294 from NHLBI and NCI; a contract HHSH234200637015C with Health Resources and Services Administration (HRSA/DHHS); two Grants N00014-12-1-0142 and N00014-13-1-0039 from the Office of Naval Research. The views expressed in this thesis do not reflect the official policy or position of the National Institute of Health, the Department of the Navy, the Department of Defense, or any other agency of the U.S. Government.

**Dedication**

This thesis is dedicated to all of my mentors who have given their time and effort to help me succeed. Without their expertise, guidance and mentorship this project would not have been possible: Julie A. Ross, PhD, MPH (University of Minnesota, Department of Pediatrics, Division of Pediatric Epidemiology and Clinical Research), Michael R. Verneris, MD (University of Minnesota, Department of Pediatrics, Division of Blood and Marrow Transplantation), Troy C. Lund, MD/PhD (University of Minnesota, Department of Pediatrics, Division of Blood and Marrow Transplantation), Daniel A. Vallera, PhD (University of Minnesota, Department of Therapeutic Radiology-Radiation Oncology) and Jeffery S. Miller, MD (Department of Medicine, Division of Hematology, Oncology and Transplantation).

**Abstract**

Myelodysplastic syndromes (MDS) are stem cell disorders that can progress to acute myeloid leukemia (AML). While hematopoietic cell transplantation (HCT) can be curative, additional therapies are needed for a disease that disproportionally afflicts the elderly. We tested the ability of a CD16xCD33 bispecific killer cell engager (BiKE) to induce natural killer (NK) cell function from 67 MDS patients. Compared to age-matched normal controls, $CD7^+$ lymphocytes, NK cells, and CD16 expression were markedly decreased in MDS patients. Despite this, reverse-antibody dependent cell-mediated cytotoxicity (R-ADCC) assays showed potent degranulation and cytokine production when resting MDS-NK cells were triggered with an agonistic CD16 mAb. Blood and marrow MDS-NK cells treated with BiKE significantly enhanced degranulation, TNF-$\alpha$ and IFN-$\gamma$ production against HL-60 and endogenous $CD33^+$ MDS targets. MDS patients had a significantly increased proportion of immunosuppressive $CD33^+$ myeloid derived suppressor cells (MDSC) that negatively correlated with MDS lymphocyte populations and CD16 loss on NK cells. Treatment with the CD16xCD33 BiKE successfully reversed MDSC immunosuppression of NK cells and induced MDSC target cell lysis. Lastly, the BiKE induced optimal MDS-NK cell function irrespective of disease stage. Our data suggest that the CD16xCD33 BiKE functions against both $CD33^+$ MDS and MDSC targets and may be therapeutically beneficial for MDS patients.

**Table of Contents**

**List of Tables**

**List of Figures**

## INTRODUCTION

MDS are clonal heterogeneous stem cell disorders characterized by normal or hypercellular bone marrow (BM) with peripheral blood (PB) cytopenias and an increased risk of progressing to frank AML[1]. The only curative treatment for MDS is HCT, although many patients are ineligible due to advanced age (median age at diagnosis is 70-75 years)[1], performance status and comorbidities. Accordingly, alternative therapies are offered, but due to the heterogeneous nature of MDS overall responses and duration of responses are suboptimal[2]. As a result, new therapeutic strategies are urgently needed to reduce MDS burden and improve overall survival.

The ability of NK cells to control human hematologic malignancies has been increasingly recognized. Consequently, NK cells are acknowledged to play an important role in tumor immunosurveillance[3-5]. NK cell function is regulated by a repertoire of inhibitory and activating surface receptors[6]. NK cell killing can occur by distinct mechanisms that involve NKG2D and natural cytotoxicity receptors (NCR), which mediate natural cytotoxicity, or through the potent activating receptor CD16 (FcγRIII) that mediates antibody dependent cell-mediated cytotoxicity (ADCC)[6-8]. NK cells from MDS patients show impairments in both natural cytotoxicity and cytokine production[9-11]. However, the ability of MDS-NK cells to function through CD16 to induce an ADCC response has not been investigated.

The therapeutic potential of manipulating NK cell function via CD16 for the treatment of cancer has been demonstrated through the use of monoclonal antibody (mAb) therapies[12,13]. Currently, novel single chain fragment variable (scFv) recombinant reagents termed bispecific and trispecific killer cell engagers (BiKE and TriKE), which specifically target CD16 expressed on effector NK cells and antigens-of-interest on tumor cells, are being developed and tested for clinical use[14-18]. We recently developed a novel BiKE that targets CD16 along with the myeloid differentiation antigen CD33 (CD16xCD33) and demonstrated its ability to facilitate effective NK cell elimination of primary $CD33^+$ AML targets[16]. Here, we tested the CD16xCD33 BiKE using primary MDS patient samples. We show that CD16 function is intact in MDS patients and can induce BiKE-mediated NK cell killing of $CD33^+$ MDS targets and $CD33^+$ immunosuppressive MDSC targets. Our data demonstrate the therapeutic potential of the CD16xCD33 BiKE and suggest that this reagent may be efficacious in patients with MDS.

## METHODS

### Patient and Clinical Data Collection

Patient samples, demographics and MDS pathology details were supplied by the NMDP and CIBMTR. De-identified samples and healthy controls were approved by the University of Minnesota institutional review board in accordance with Declaration of Helsinki. Pathologic classification data were available in the FAB format (RA, RARS, RAEB, RAEB-T, and CMML), which shows the overlap between MDS and AML. Raw

cytogenetic data were available in the majority of patients (n=48). We further sub-classified the raw cytogenetic data into the defined international prognosis scoring system (IPSS) classification categories of favorable (-Y, 20q, 5q-), poor (complex (≥3 abnormalities) or chromosome 7 abnormalities), or intermediate (all others). Blast percentage at the time of transplant was also available and categorized by IPSS classification.

**Cell Isolation**

Peripheral blood mononuclear cells (PBMC) from MDS patients were collected pre-transplant, prior to treatment and cryopreserved by the NMDP Research Repository. PBMC from age-matched normal donors (median age: 59 years, range: 22-80, 44% female, 56% male) were isolated from adult blood obtained from Memorial Blood Center (Minneapolis, MN) by centrifugation using a Histopaque gradient (Sigma-Aldrich, St. Louis, MO) and cryopreserved. Paired blood and marrow samples were obtained from the Leukemia Tissue Bank, a shared resource at the University of Minnesota. All samples were obtained after informed consent, using guidelines approved by the Committee on the Use of Human Subjects in Research at the University of Minnesota and the NMDP in accordance with the Declaration of Helsinki.

**Cell Lines**

The $CD33^+$ human acute promyelocytic leukemia cell line HL-60 (ATCC, Manassas, VA) was cultured at 37°C with 5% $CO_2$ in Iscove's medium (Invitrogen, Carlsbad, CA)

supplemented with 20% FBS (Gibco-Invitrogen) and 100U/mL penicillin and 100U/mL streptomycin (Invitrogen). The murine mastocytoma cell line P815 (ATCC) was cultured at 37°C with 5% $CO_2$ in Dulbecco's Modified Eagle's Medium (DMEM), high glucose (Invitrogen) supplemented with 10% FBS and 100U/mL penicillin and 100U/mL streptomycin.

**Cytokine-Derived MDSC Targets**

*In vitro* generation and characterization of cytokine-derived human MDSC targets from normal PBMC were performed as previously described[19]. The phenotype of *in vitro* cytokine-derived MDSC was evaluated by flow cytometry for the expression of CD45, CD33, CD11b, CD14 and HLA-DR. qRT-PCR was used for the evaluation of specific, differentiation-associated gene expression as previously described[19]. The ability to suppress the proliferation of CFSE-labeled (Invitrogen) allogeneic T and NK cells in 5 day MDSC-co-cultures (effector:target (E:T) ratio = 1:2) was evaluated by flow cytometry as previously described[19].

**Flow Cytometry**

Cells were immunophenotyped with the following fluorescent-labeled monoclonal antibodies (mAb) against: PE-Cy7-conjugated CD56 (HCD56; BioLegend, San Diego, CA), ECD-conjugated CD3 (UCHT1; Beckman Coulter, Brea, CA), APC-Cy7-conjugated CD16 (3G8; BioLegend), PE-conjugated CD7 (M-T701; BD Biosciences, San Jose, CA), Pacific Blue-conjugated CD45 (HI30; BioLegend), FITC-conjugated CD2

(S5.2; BD Biosciences), PerCP-Cy5.5-conjugated anti-human CD107a (LAMP-1) (H4A3; BioLegend), Pacific Blue-conjugated anti-human IFN-γ (4S.B3; BioLegend), FITC-conjugated TNF-α (MAb11; BioLegend), FITC-conjugated CD33 (P67.6; BD Biosciences), PE-conjugated CD11b/Mac-1 (ICRF44; BD Biosciences), APC-Cy7-conjugated CD14 (M5E2; BioLegend), PE-Cy5-conjugated HLA-DR (L243; BioLegend) and APC-conjugated CD45 (HI30; BioLegend). Phenotypic acquisition of cells was performed on the LSRII (BD Biosciences) and analyzed with FlowJo software (Tree Star Inc., Ashland, OR).

**Construction, Expression and Purification of the bscFv CD16xCD33 BiKE**

The synthesis and assembly of hybrid genes encoding the CD16x33 BiKE reagent were accomplished by using DNA shuffling and DNA ligation techniques as previously described[16,20,21]. DNA-sequencing analysis (Biomedical Genomics Center, University of Minnesota) was used to verify that the gene was correct in sequence and cloned in frame. For bacterial protein expression and purification by ion exchange and size exclusion chromatography, methods were used as previously described[20].

**Cytokine/Chemokine Production and Degranulation (CD107a) Assay**

Thawed PBMC from MDS patients and normal donors were incubated overnight at 37ºC, 5% $CO_2$ in basal medium or basal medium supplemented with IL-12 (10ng/mL) and IL-18 (100ng/mL). Cells were then treated with the CD16xCD33 BiKE (10μg/mL), scFvCD16 control reagent (10μg/mL) or no reagent, co-cultured with (E:T ratio = 10:1)

or without HL-60 or cytokine-derived MDSC targets and CD107a expression and intracellular IFN-γ and TNF-α production were evaluated as previously described[16].

**51-Chromium Release Cytotoxicity Assay**

Cytotoxicity was evaluated by 4-hour $^{51}$Cr-release assays. Briefly, resting PBMC from normal donors treated with the CD16xCD33 BiKE (10μg/mL), scFvCD16 control reagent (10μg/mL) or no reagent were co-cultured for 4-hours with $^{51}$Cr-labeled cytokine-derived MDSC or HL-60 targets at varying E:T ratios. $^{51}$Cr release was measured by a gamma scintillation counter (Perkin Elmer, Walthman, MA) and specific target lysis was determined[16].

**Reverse Antibody Dependent Cell-Mediated Cytotoxicity (R-ADCC) Assay**

Resting PBMC from MDS patients and normal donors were coated with 10μg/mL of the following agonistic mAb in various combinations for 30 minutes at room temperature: anti-CD16 (3G8; BioLegend), anti-DNAM-1 (11A8; BioLegend), anti-CD2 (TS1/8; BioLegend), anti-2B4 (C1.7; BioLegend) and mIgG (MOPC-21; BioLegend). Coated PBMC were then co-cultured with P815 targets in basal medium for 4 hours at 37°C with 5% $CO_2$ and CD107a expression and intracellular IFN-γ and TNF-α production were evaluated as previously described[16].

**Statistical Analysis**

Grouped data were expressed as mean ± standard error mean (SEM). Differences between two groups were analyzed by Student's *t* test or the Mann-Whitney test. Differences between more than two groups were analyzed by two-way analysis of variance (ANOVA) followed by Bonferroni's or Tukey-Kramer's post-tests. Spearman's rho tests were used to evaluate correlative relationships (GraphPad Prism Statistical Software, La Jolla, CA).

## RESULTS

### MDS Patient Characteristics

MDS patient samples were collected pre-transplant, prior to treatment from a cohort undergoing adult unrelated donor allogeneic transplantation. Among the 67 MDS patients, 60% were male and 40% were female with a median age of 47 years (range, 19-74). According to FAB classification 13% had refractory anemia (RA), 12% RA with ringed sideroblasts (RARS), 36% refractory anemia with excess blasts (RAEB), 15% refractory anemia with excess blasts in transformation (RAEB-T) and 24% were classified as other (Appendix Table 1). Based on data available from the era of sample collection (1990-2005), 48 patients had cytogenetic data available and could be stratified by an IPSS cytogenetic classification (36% of patients had a favorable karyotype, 15% intermediate and 22% poor) and 57 patients had blast percentage at date of transplant data available and could be stratified by IPSS categories (52% of patients had <5% blasts, 21% had 5-10% blasts, 4% had 11-20% blasts and 8% had ≥21% blasts).

**NK cells and their CD16 expression are significantly decreased in MDS patients**

PBMC populations from normal donors and MDS patients were analyzed by flow cytometry to determine the frequencies of $CD7^+$ lymphocytes, $CD56^-/CD3^+$ T cells, $CD56^+/CD3^+$ NKT cells and $CD56^+/CD3^-$ NK cells (Figure 1A and 1B). Compared to normal donors, MDS patients had a significant decrease in $CD7^+$ lymphocytes, T and NK cells while no significant difference was observed for the NKT population (Figure 1C, Appendix Figure 1A and Table 1). Further evaluation of the NK cell $CD56^{bright}$ and $CD56^{dim}$ subpopulations did not reveal any significant differences between normal donors and MDS patients (Table 1). CD16 expression was significantly decreased on MDS NK cells compared to normal donor PB-NK cells (Percent: 63±3% vs. 89±2%; MFI: 1169±177 vs. 5470±656; $p < 0.0001$; Figure 1D and Appendix Figure 1B).

**Activation of NK cells through CD16 is intact in MDS patients**

An agonistic mAb against CD16 was used to induce NK cell function in a R-ADCC assay. Compared to the IgG control, CD16 crosslinking of resting MDS-NK cells led to a significant increase in degranulation (16±2% vs. 46±5%, $p < 0.0001$, n=16), which was similarly observed in normal donors (11±1% vs. 46±3%, $p < 0.0001$, n=12; Figure 2A). Intracellular cytokine production induced via CD16 triggering was evaluated and a comparison of MDS patients to normal donors did not show any significant differences in TNF-α (MDS: 9±2% vs. normal: 6±1%, $p = 0.331$; Figure 2B) or IFN-γ (6±1% vs. 10±2%, $p = 0.113$; Figure 2C) production further demonstrating the ability of MDS-NK cells to function through CD16 despite the lower expression levels. Activation of resting

NK cells occurs via synergistic interactions between CD16 and the co-activating receptors DNAM-1, CD2 and 2B4[22]. To further evaluate the function of CD16 on MDS-NK cells, CD16 was co-crosslinked in pairwise combinations and function was measured. Compared to the IgG control, all receptor combinations with CD16 induced significant increases in CD107a expression (Figure 2A), TNF-α (Figure 2B) and IFN-γ (Figure 2C) production in MDS-NK cells. No significant differences in degranulation and TNF-α production induced by co-crosslinking receptor pairs were observed between normal donors and MDS patients. However, MDS-NK cells displayed a significant decrease in IFN-γ production compared to normal donor NK cells for CD16 crosslinking combinations with DNAM-1, CD2 and 2B4. No differences in DNAM-1, CD2 and 2B4 receptor expression were observed between normal donor and MDS-NK cells (Appendix Figure 2). To evaluate whether the diminished IFN-γ production by MDS-NK cells was specific to CD16 synergistic activation, resting MDS-NK cells were stimulated overnight with saturating concentrations of IL-12 and IL-18. Compared to normal donors, MDS-NK cells displayed a significant reduction in IFN-γ production in response to cytokine stimulation (Appendix Figure 3) revealing a broader defect in the activation threshold for the IFN-γ pathway.

**CD16xCD33 BiKE enhances NK cell activity against primary CD33$^+$ MDS targets**

To evaluate the therapeutic potential of targeting CD16 in MDS patients, PBMC from normal donors and MDS patients were treated with the CD16xCD33 BiKE, scFv CD16 control or no reagent and co-cultured with the CD33$^+$ HL-60 cell line. NK cell

degranulation and TNF-α and IFN-γ production were then evaluated by flow cytometry. Compared to the no reagent and scFv CD16 controls, MDS-NK cell degranulation (Figure 3A), TNF-α (Figure 3B) and IFN-γ (Figure 3C) production were significantly increased. Moreover, in the absence of HL-60 targets, MDS-NK cells treated with the CD16xCD33 BiKE targeted endogenous $CD33^+$ cells, significantly enhancing degranulation (Figure 3D) and TNF-α (Figure 3E) and IFN-γ (Figure 3F) production. As with CD16 synergistic crosslinking and IL-12 and IL-18 stimulation, CD16xCD33 BiKE stimulation of MDS-NK cells resulted in lower levels of IFN-γ production in the presence (Figure 3C) and absence (Figure 3F) of HL-60 targets compared to normal donors.

**The $CD33^+$ MDSC population is significantly increased in MDS patients and negatively correlates with MDS lymphocyte populations**

Suppressive MDSC are phenotypically defined as $CD33^+/CD11b^+/CD14^-/HLA\text{-}DR^{lo/-}$ and are increased during oncogenesis and in the presence of inflammatory cytokines[23]. We, therefore, evaluated the presence of MDSC in MDS. Within the all cell fraction, the total $CD33^+$ cell population frequency was significantly higher in MDS patients compared to normal donors (29±2% vs. 16±2%, $p = 0.002$; Table 1). $CD7^+$ lymphocytes, T and NK cells from normal donors and MDS patients lacked expression of CD33 (Appendix Figure 4A-4E). Additional sub-gating within the $CD33^+$ fraction showed a distinct MDSC population in MDS patients that was not observed in normal donors (Appendix Figure 5), where MDS-MDSC comprised 21±2% of the total $CD33^+$ cell fraction (vs. normal: 0.7±0.1%, $p < 0.0001$) and 6±1% of the all cell fraction (vs.

0.1±0.02%, $p < 0.0001$; Figure 4A). The relationships between MDSC and lymphocyte populations were next evaluated in MDS patients. Among all MDS patients, there was a statistically significant negative correlation between percent MDSC and percent $CD7^+$ lymphocytes, T cells, NKT cells and NK cells (Figure 4B). Interestingly, when stratifying the MDS patients by disease status, a statistically significant stronger negative correlation was observed between MDSC and NK cells ($r = -0.6104$, $p < 0.01$) for lower risk MDS patients, whereas no significant correlations were observed for $CD7^+$ lymphocytes, T and NKT cells (Figures 4C). Among higher risk MDS patients there were significant negative correlations between MDSC and $CD7^+$ lymphocytes, T and NKT cell populations (Figure 4D). Moreover, a statistically significant negative correlation between MDS-MDSC and MDS-NK cell CD16 expression was also observed (Appendix Figure 6), suggestive of a MDSC immunosuppressive mechanism against NK cells. Taken together, these findings support a negative relationship between the MDSC population and lymphocyte populations in MDS patients and further support the evidence that immunosuppressive MDSC help facilitate ineffective hematopoiesis in MDS[24].

**Immunosuppressive MDSC are targeted by the CD16xCD33 BiKE**

MDSC have been shown to suppress NK cell activity[25,26], therefore, we next evaluated the ability of the CD16xCD33 BiKE to activate NK cells in the presence of immunosuppressive MDSC. Cytokine-derived MDSC were generated from PBMC isolated from normal donors and post-induction characterization analysis verified the MDSC phenotype and gene expression signature (data not shown). Cytokine-derived

MDSC functioned to suppress T cell (Appendix Figure 7A) and NK cell proliferation (Figure 5A). The MDSC targets were then labeled with $^{51}Cr$ and co-cultured with normal donor resting NK cells in the absence or presence of the CD16xCD33 BiKE or scFv CD16 control. Without reagent treatment or when treated with the scFv CD16 control, NK cell cytotoxicity was suppressed in the presence of MDSC targets. However, when treated with the CD16xCD33 BiKE, there was a significant increase in MDSC killing (CD16xCD33 BiKE vs. no reagent: (20:1) 63±5% vs. 7±2%, $p < 0.0001$; Figure 5B). Evaluation of NK cell degranulation and intracellular cytokine production revealed significant increases in CD107a expression (Figure 5C), TNF-α (Figure 5D) and IFN-γ (Figure 5E) production as well in the presence of MDSC targets when resting NK cells were treated with the CD16xCD33 BiKE. We next evaluated the ability of the CD16xCD33 BiKE to enhance PB and BM MDS-NK cell function against MDSC targets. Significant increases in degranulation (Figure 5F), TNF-α (Figure 5G) and IFN-γ (Figure 5H) production were observed in the presence of the BiKE. Similar results were found using HL-60 targets (Appendix Figures 7B-7D). Notably, no significant differences were observed between PB and BM MDS-NK cell BiKE-mediated function. Overall, these data demonstrate the ability of the CD16xCD33 BiKE to induce blood and marrow MDS-NK cell activation to overcome MDSC immunosuppression.

**CD16xCD33 BiKE-enhanced NK cell activity functions regardless of MDS disease stage**

MDS is a heterogeneous disease and treatment options depend on several clinical factors specific to each patient. Therefore, the ability of the CD16xCD33 BiKE to enhance NK cell function among the various MDS groups stratified by clinical features was evaluated. No significant differences in NK cell (Figure 6A), total $CD33^+$ (Figure 6B) and MDSC (Figure 6C) population frequencies were observed among FAB classification and IPSS karyotype groups in MDS patients. Upon evaluation of CD16xCD33 BiKE-induced MDS-NK cell function (degranulation, TNF-$\alpha$ and IFN-$\gamma$ production) in the absence of HL-60 targets (Figure 6D) and in the presence of HL-60 targets (Figure 6E), no significant differences between MDS groups were observed. Stratifying by blast percentage also showed no significant differences in the study variables (Appendix Table 2). As the median age of our patient cohort indicated a younger population, respectively, the study variables were also stratified by age to evaluate a potential age effect. No significant differences were observed in percent NK cells, total $CD33^+$ cells, MDSC or CD16xCD33 BiKE-induced NK cell function among age strata in MDS patients (Appendix Figure 8). Altogether these data indicate that despite disease heterogeneity, the CD16xCD33 BiKE can consistently function to enhance MDS-NK cell activity against the $CD33^+$ target cell population, which includes immunosuppressive MDSC, regardless of disease stage.

## DISCUSSION

We examined the expression and function of CD16 on MDS-NK cells and the ability of a CD16xCD33 BiKE to mediate MDS-NK cell targeting of the $CD33^+$ cell population that

contains both the premalignant clone and immunosuppressive MDSC. Previous studies of MDS-NK cells from PB and BM have evaluated NK cell function in the context of natural cytotoxicity mediated by NKp46, NKp30, NKG2D, 2B4 and DNAM-1[9-11]. Kiladjian et al. described decreased cytolytic function of PB NK cells from all MDS subtypes against K562 targets despite normal expression of natural cytotoxicity receptors, as well as decreased IFN-γ and TNF-α secretion in response to IL-2 stimulation[9]. In contrast, Epling-Burnette et al. observed down-regulation of NKp30 and NKG2D and correlated PB MDS-NK cell dysfunction with decreased NKG2D expression[10]. In another study, Carlsten et al. found significant decreases in DNAM-1 and NKG2D expression in BM MDS-NK cells that were not observed in PB MDS-NK cells; despite this difference, both sources of MDS-NK cells displayed impaired degranulation in the presence of K562 cells and in a R-ADCC assay triggering through NKG2D, 2B4 and DNAM-1[11]. Our study demonstrated that despite reduced CD16 expression on MDS-NK cells, degranulation and TNF-α and IFN-γ production could be induced through CD16 stimulation by an agonistic mAb and the CD16xCD33 BiKE, indicating a functional ADCC response in MDS patients. This agrees with early evidence that showed an intact lymphocyte ADCC response in patients with primary preleukemic syndrome (PPS) while abnormalities in other lymphocyte functions were observed[27]. Notably, when we co-crosslinked MDS-NK cells with pairwise combinations of CD16 and co-activating receptors, synergistic activation was significantly diminished for IFN-γ production, but not degranulation or TNF-α production. Decreases in IFN-γ production were also found when MDS-NK cells were stimulated with IL-12 and IL-18 and the CD16xCD33 BiKE.

Our data agree with previous work that showed decreased NK cell IFN-γ production despite stimulation with IL-12 and IL-18 in the context of a murine hepatic tumor model containing immunosuppressive MDSC[25]. Importantly, however, we demonstrate cytotoxicity was not impaired in MDS patients and could be driven by CD16xCD33 BiKE stimulation. Fauriat et al. has demonstrated that NK cell IFN-γ production has a greater threshold of activation than that of degranulation and TNF-α production[28]. Our data, therefore, suggest NK cell functions that have a lower threshold of activation are intact in MDS patients while the higher activation threshold required for stimulation of the IFN-γ pathway may be impaired.

Increases in the frequency of circulating MDSC have been well described in solid tumors and studies have shown MDSC are an important factor in facilitating immune evasion and tumor progression[23,29-32]. While the roles of MDSC in hematologic malignancies are still evolving, a recent study demonstrated an increase in MDSC frequency in the PB of multiple myeloma (MM) patients that increased with disease progression and promoted tumor growth via suppression of $CD4^+$ T, $CD8^+$ T and NKT cell lymphocyte populations[33]. We demonstrated here that the percent of MDSC is significantly increased in the PB of MDS patients and negatively correlates with $CD7^+$ lymphocytes, T, NKT and NK cell populations. Interestingly, when MDS patients were stratified by disease status, this negative relationship was only significant for NK cells in patients with lower risk. By contrast, the negative correlations between MDSC and total lymphocytes, T and NKT cells were significant for patients with higher risk. MDSC are generated from

immature myeloid cells, which includes immature dendritic cells (DC)[23]. The crosstalk between NK cells and DC has been well studied and it has been shown that NK cells play a role in DC maturation via the secretion of TNF-α and IFN-γ as well as cell-to-cell contact mechanisms that involve NKp30[34-37]. Expansion and activation of MDSC require several different factors that include TNF-α and IFN-γ[38-41]. As our data show a statistically significant negative correlation between MDSC and NK cells for lower risk disease, it is possible the altered BM microenvironment in MDS primes the induction and expansion of immature DC to MDSC and interaction with NK cells promotes MDSC functional activation via NK cell secretion of TNF-α and IFN-γ, which in turn ultimately leads to suppression of the enabling NK cells. Moreover, studies have shown activated MDSC promote the development and expansion of T regulatory ($T_{reg}$) cells[42-44], which is a characteristic of MDS patients with advanced disease[45-47]. This supports our data showing a statistically significant negative correlation between MDSC and T cells in MDS patients with higher risk. Taken together, these data suggest a potential model whereby interactions early in disease between MDSC-primed immature myeloid cells and NK cells promote the functional activation of MDSC, leading to suppression of this innate lymphocyte population and promotion of $T_{reg}$ cell development, which ultimately function in concert with MDSC to suppress adaptive immunity and facilitate disease progression. Further studies are underway to investigate this hypothesis.

MDSC use multiple mechanisms to suppress antitumor immunity. Down-regulation of L-selectin (CD62L) on T cells has been shown to impair T cell homing to lymph nodes and

activation[23]. Hanson et al. demonstrated MDSC constitutively express the sheddase ADAM 17 (a disintegrin and metalloproteinase domain 17) on their plasma membrane and suggest ADAM 17 is the enzyme responsible for cleaving the ectodomain of L-selectin[48]. We recently demonstrated that NK cell CD16 surface expression is regulated by ADAM 17, which functions to promote attenuation of NK cell function through cleavage of CD16 from the cell surface[49]. We show here a statistically significant negative correlation between MDSC and MDS-NK cell expression of CD16 suggesting a novel role for MDSC suppression of NK cell function, namely the induction of NK cell CD16 shedding. Accordingly, further testing of an ADAM 17 inhibitor in combination with the CD16xCD33 BiKE in MDS is warranted and may further serve to inhibit MDSC immunosuppression and enhance NK cell effector function against $CD33^+$ targets.

Immune suppression has a crucial role in promoting tumor progression and the supporting data clearly indicate that elimination of suppressing factors is required for cancer immunotherapies to be successful[50]. Our data and others suggest that MDSC contribute to ineffective hematopoiesis in MDS[24]. Thus, the ability to target this immunosuppressive population through the CD16xCD33 BiKE may be therapeutically beneficial for patients with MDS and other diseases characterized by increased MDSC. Acknowledging that the CD16xCD33 BiKE can also target normal $CD33^+$ cells (monocytes and committed myeloid progenitors), transient myelosuppression may be expected with this therapy, not unlike most cytotoxic therapies. Clinical trials show CD3xCD19 BiTE therapy is efficacious for ALL while targeting of the normal cell

compartment is well tolerated[51-53]. This is in part due to the ease with which drug exposure can be managed; an important feature that helps control on-target/off-tumor effects allowing regeneration of the normal cell compartment after drug elimination. Moreover, for NK cells, other receptor-ligand interactions, facilitated by the BiKE-mediated effector-target cell synapse, may play an important role in target cell elimination. In conclusion, we propose that CD16xCD33 BiKE is a promising therapy for MDS and other myeloid malignancies.

**TABLES**

## Table 1: Summary of MDS PBMC Population Frequencies

| | Normal | MDS | *P*-value |
|---|---|---|---|
| Sample Size (n) | 20 | 67 | |
| | | | |
| [a]$CD45^+/SSC^{lo}$ (Non-myeloid) | 74 ± 2% | 50 ± 2% | **<0.0001** |
| [a]$CD45^+/CD7^+$ Lymphocytes | 54 ± 3% | 25 ± 2% | **<0.0001** |
| [a]$CD56^+/CD3^-$ NK Cells | 6 ± 1% | 2 ± 0.3% | **<0.0001** |
| [b]$CD56^{+bright}/CD3^-$ NK Cells | 9 ± 2% | 10 ± 2% | 0.84 |
| [b]$CD56^{+dim}/CD3^-$ NK Cells | 90 ± 2% | 89 ± 2% | 0.85 |
| [a]$CD56^+/CD3^+$ NKT Cells | 1 ± 0.2% | 1 ± 0.1% | 0.61 |
| [a]$CD56^-/CD3^+$ T Cells | 40 ± 3% | 20 ± 2% | **<0.0001** |
| | | | |
| [a]$CD45^+/SSC^{hi}$ (Myeloid) | 21 ± 2% | 36 ± 3% | **0.001** |
| [a]$CD33^+$ | 16 ± 2% | 29 ± 2% | **0.002** |
| [a]MDSCs ($CD33^+/CD11b^+/CD14^-/HLA\text{-}DR^{lo/-}$) | 0.1 ± 0.02% | 6 ± 1% | **<0.0001** |

[a]Percent of all cells based on FSC/SSC gate excluding debris
[b]Percent of $CD7^+/CD56^+/CD3^-$ NK cell population

**FIGURES**

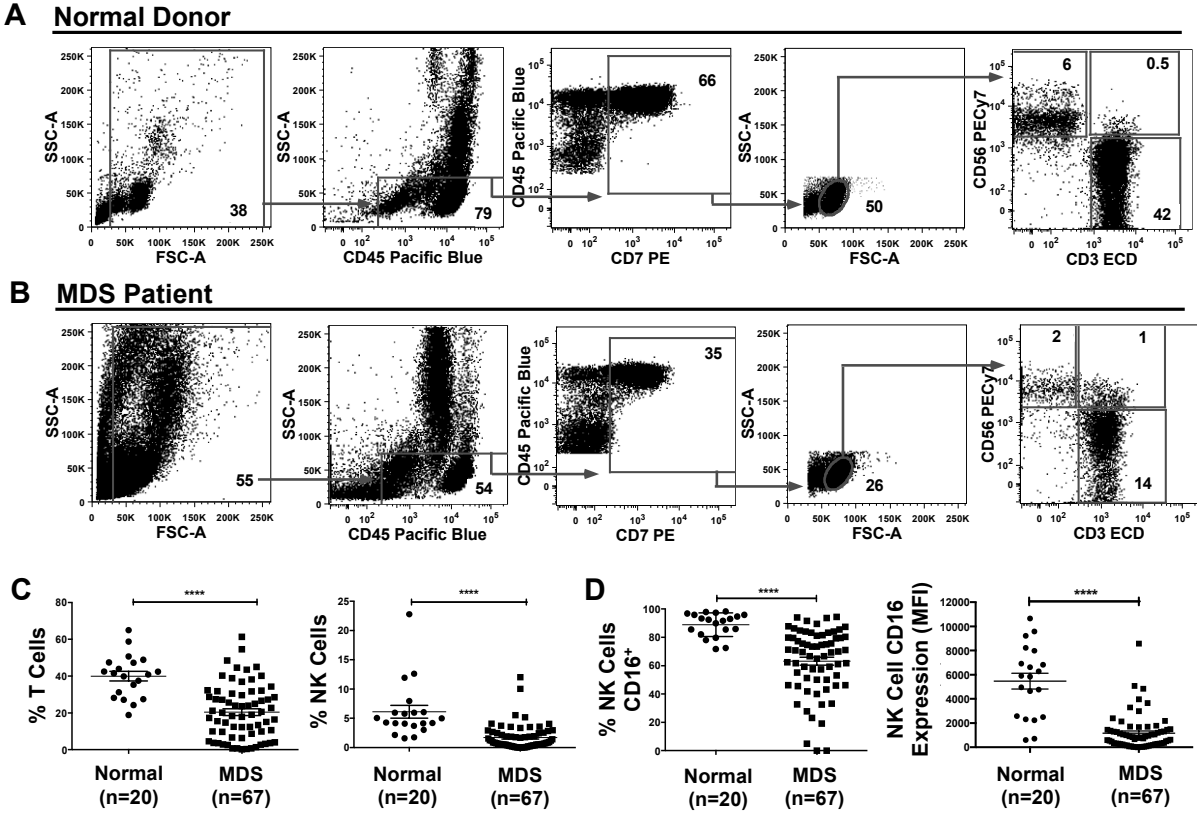


**Figure 1: Aberrant NK cell frequency and NK cell CD16 expression in MDS PBMC.**
(A-C) PBMC from normal donors and MDS patients were stained with anti-CD56, anti-CD3, and anti-CD16 mAbs. (A-B) Gating strategy for the evaluation of the lymphocyte populations in normal donors (A) and MDS patients (B). Plots are representative from one normal donor (#12 of 20) and one higher risk MDS patient (#49 of 67) and gate frequency indicates population percent normalized to the all cell fraction based on the FSC/SSC gate excluding debris. (C) Percent of $CD56^{-}/CD3^{+}$ T cells and $CD56^{+}/CD3^{-}$ NK cells (normalized to all cell fraction based on the FSC/SSC gate excluding debris) and (D) percent of $CD16^{+}$ NK cells (calculated as the percent of $CD56^{+}/CD3^{-}$ NK cells) as well as Mean Fluorescence Intensity (MFI) of CD16 expression on NK cells were determined by FACS analysis (****$P$<0.0001).

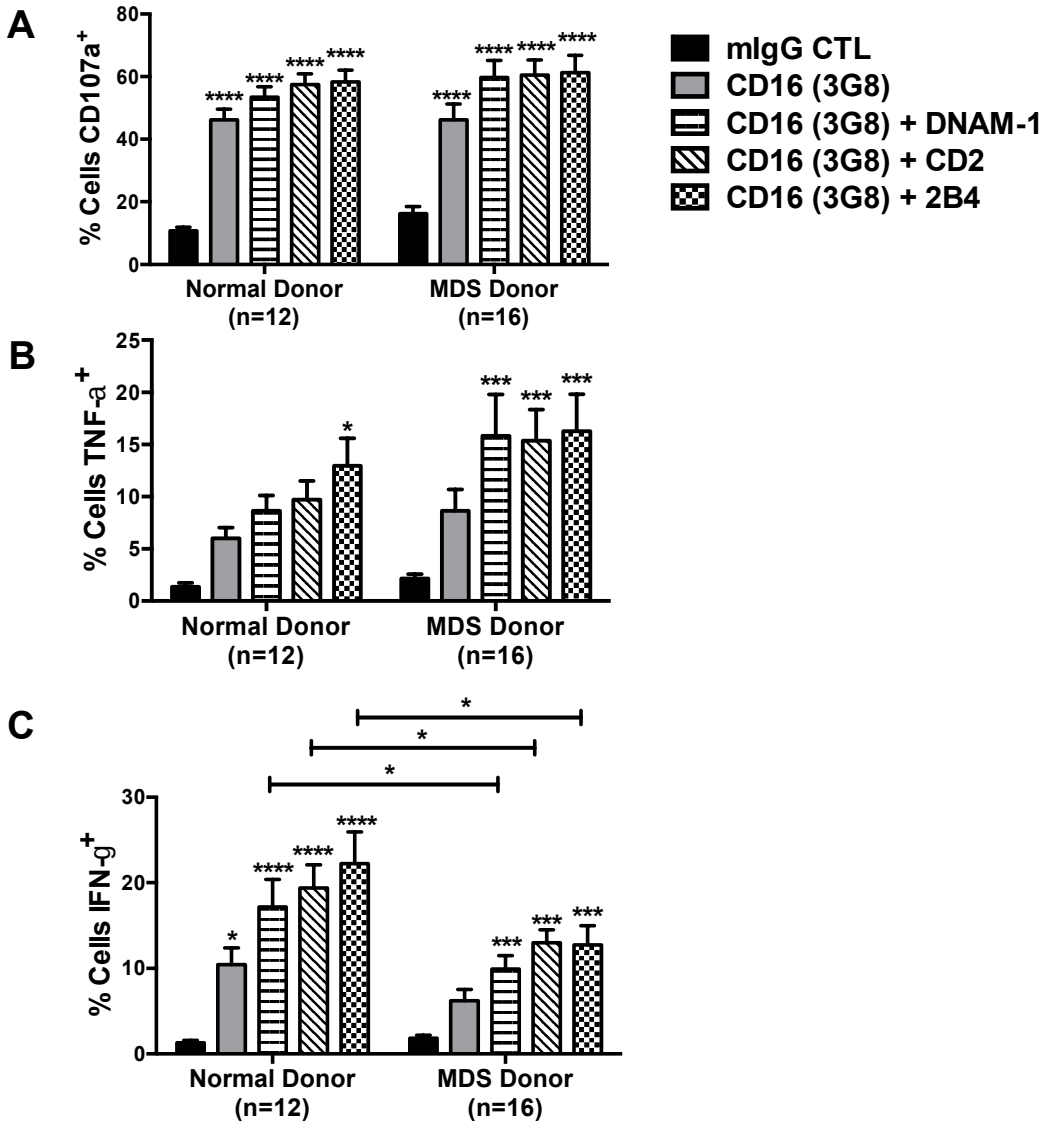


**Figure 2: NK cell activation induced through CD16 crosslinking is intact in MDS-NK cells.** (A-C) Resting PBMC from normal donors and MDS patients were coated with 10μg/mL of the indicated mAbs, co-cultured with P815 targets and a R-ADCC assay was performed. NK cell CD107a expression (A) and intracellular TNF-α (B) and IFN-γ (C) production were evaluated by FACS analysis (**P*<0.05, ****P*<0.001, *****P*<0.0001).

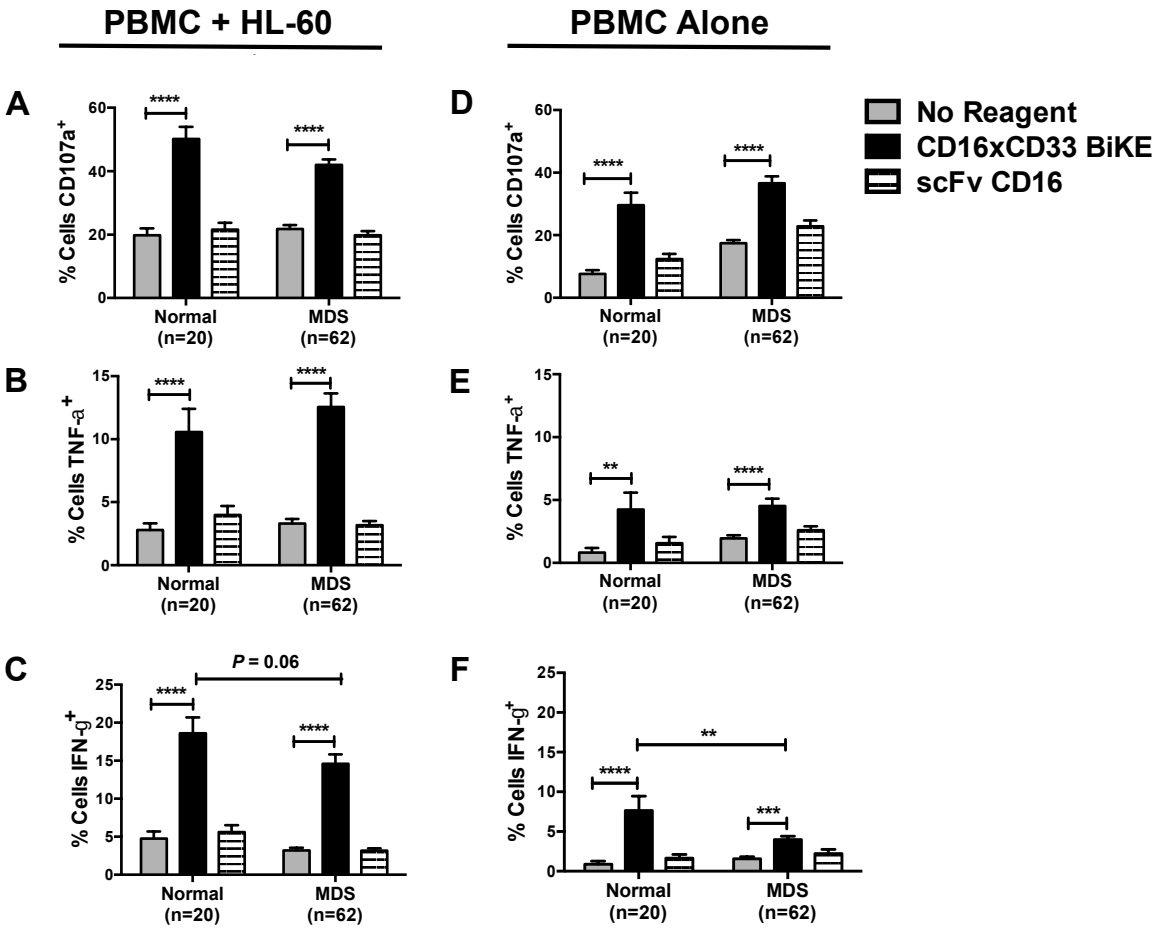


**Figure 3: CD16xCD33 BiKE enhances MDS-NK cell function against CD33$^+$ targets.**
(A-F) Resting PBMC from normal donors and MDS patients were coated with 10μg/mL of the CD16xCD33 BiKE or scFv CD16 control and co-cultured with (A-C) or without (D-F) CD33$^+$ HL-60 targets. NK cell CD107a expression and intracellular TNF-α and IFN-γ production were evaluated by FACS analysis (**P*<0.05, ***P*<0.01, ****P*<0.001, *****P*<0.0001).

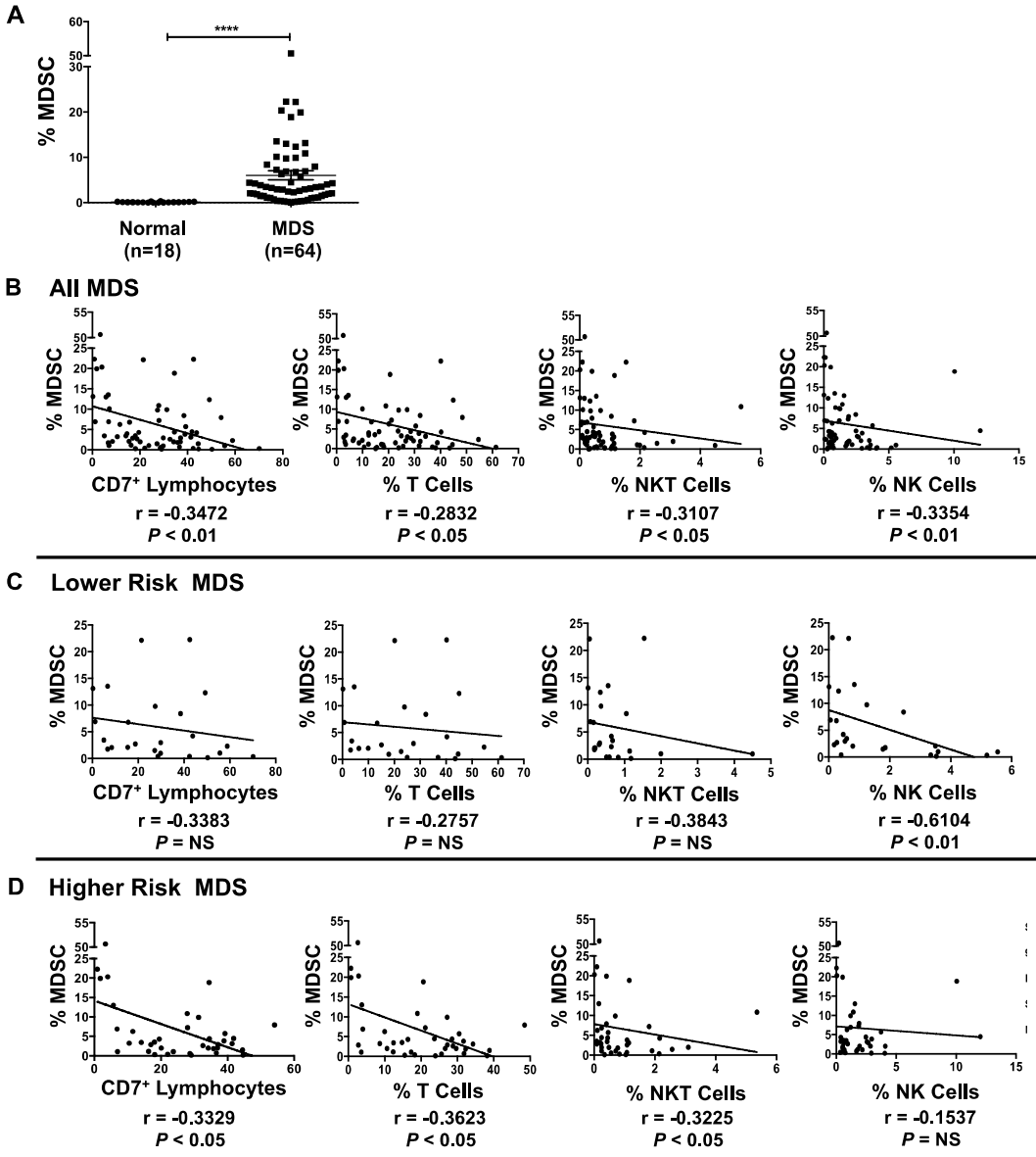


**Figure 4: MDS patients have a significant increase in MDSC that negatively correlates with lymphocyte populations.**

(A) PBMC from normal donors and MDS patients were stained with anti-CD45, anti-CD33, anti-CD11b, anti-CD14 and anti-HLA-DR mAbs and the percent of MDSC (phenotypically defined as $CD33^{+}/CD11b^{+}/CD14^{-}/HLA\text{-}DR^{lo/-}$) of the all cell fraction was evaluated (****$P$<0.0001). (B-D) Based on the all cell fraction, the correlation between % MDSC and % $CD7^{+}$ lymphocytes, % T cells, % NKT cells and % NK cells among all MDS patients (B), lower risk MDS patients (C) and higher risk MDS patients (D). Correlation coefficients (r) and statistical significance are indicated in the figure.

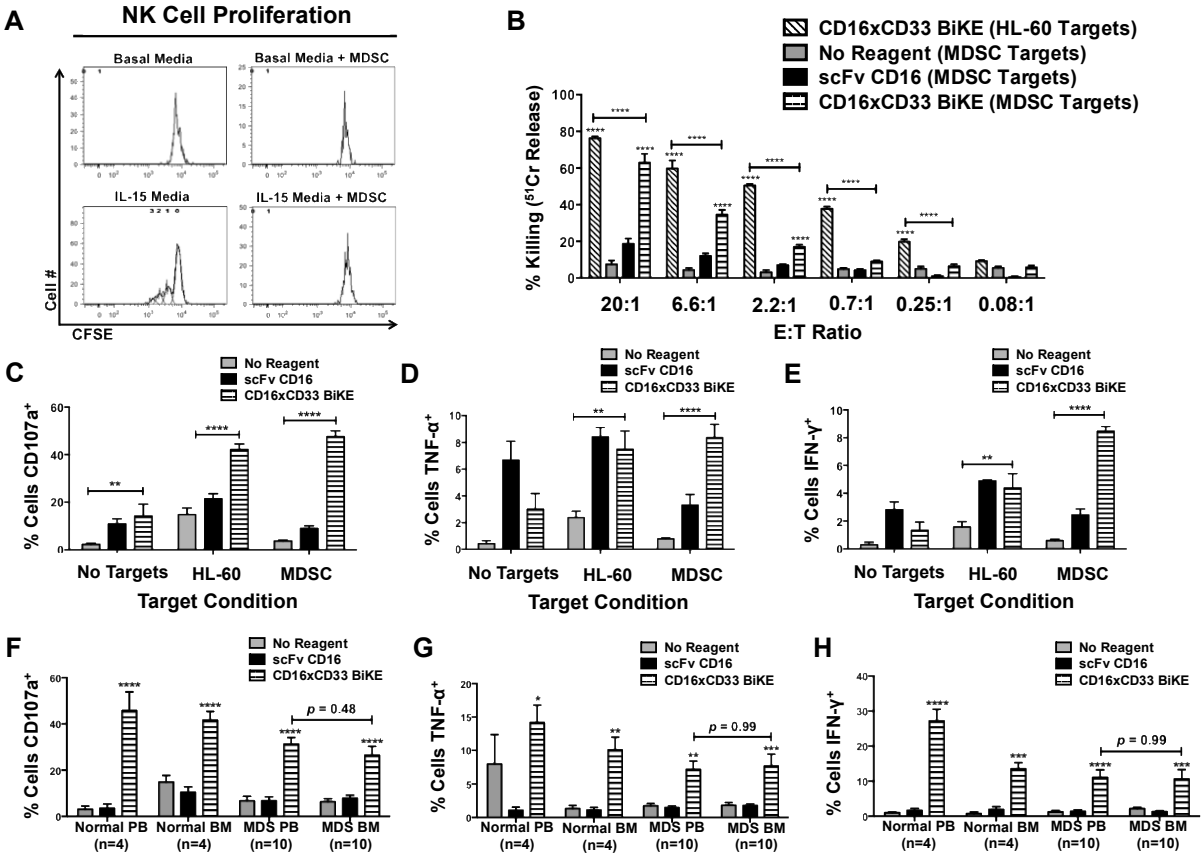


**Figure 5: CD16xCD33 BiKE enhances NK cell cytotoxicity and cytokine production against MDSC targets.**

(A) CFSE-labeled NK cells were cultured for 5 days in basal medium or medium supplemented with 10ng/mL IL-15 in the presence or absence (E:T ratio = 1:2) of cytokine-derived MDSC from normal PBMC and proliferation was evaluated via FACS analysis. Histogram plots represent one of six normal donors. (B) PBMC from normal donors were coated with 10μg/mL of CD16xCD33 BiKE or scFv CD16 control, co-cultured with cytokine-derived MDSC or HL-60 targets and NK cell-mediated cytotoxicity was evaluated via a $^{51}$Cr-release assay (****$P$<0.0001, (n=4)). (C-E) PBMC from normal donors were coated with 10μg/mL of CD16xCD33 BiKE or scFv CD16 control, co-cultured with cytokine-derived MDSC or HL-60 targets and NK cell CD107a expression and intracellular TNF-α and IFN-γ production were evaluated via FACS analysis (**$P$<0.01, ****$P$<0.0001, (n=6)). (F-H) Mononuclear cells from paired peripheral blood (PB) and bone marrow (BM) samples were isolated from normal donors (n=4) and MDS patients (n=10), coated with 10μg/mL of CD16xCD33 BiKE or scFv CD16 control, co-cultured with cytokine-derived MDSC and NK cell (F) CD107a expression and intracellular (G) TNF-α and (H) IFN-γ production were evaluated via FACS analysis (*$P$<0.05, **$P$<0.01, ***$P$<0.01, ****$P$<0.0001).

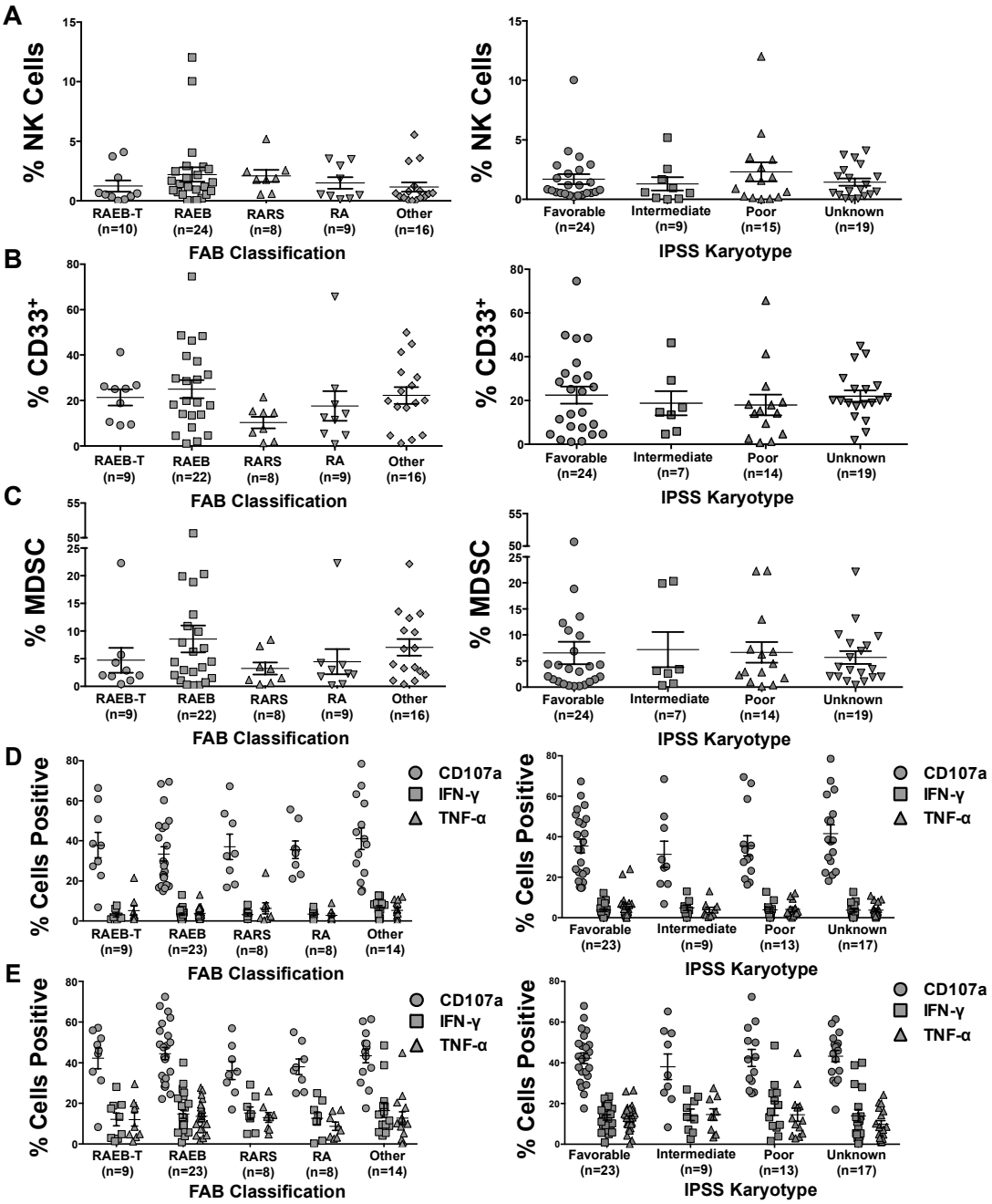


**Figure 6: CD16xCD33 BiKE consistently enhances NK cell function at all disease stages.** The percent of $CD56^{+}/CD3^{-}$ MDS-NK cells (A), total $CD33^{+}$ cells (B) and MDS-MDSC (C) of the all cell fraction was stratified according to their respective FAB classification and IPSS karyotype groups. (D-E) CD16xCD33 BiKE-induced MDS-NK cell functions (degranulation (CD107a), intracellular TNF-α and IFN-γ production) in the absence of HL-60 targets (D) and in the presence of HL-60 targets (E) were stratified according to their respective FAB classification and IPSS karyotype groups. Y-axis of graphs (D and E) represent the percent of NK cells positive for each function listed in graph legend.

## REFERENCES


1. Ma X, Does M, Raza A, Mayne ST. Myelodysplastic syndromes: incidence and survival in the United States. *Cancer*. 2007;109(8):1536-1542.
2. (NCCN) NCCN. NCCN Clinical Practice Guidelines in Oncology (NCCN Guidelines). Myelodysplastic Syndromes Version 2.2014; 2013.
3. Miller JS, Soignier Y, Panoskaltsis-Mortari A, et al. Successful adoptive transfer and in vivo expansion of human haploidentical NK cells in patients with cancer. *Blood*. 2005;105(8):3051-3057.
4. Ruggeri L, Capanni M, Casucci M, et al. Role of natural killer cell alloreactivity in HLA-mismatched hematopoietic stem cell transplantation. *Blood*. 1999;94(1):333-339.
5. Guimarães F, Guven H, Donati D, et al. Evaluation of ex vivo expanded human NK cells on antileukemia activity in SCID-beige mice. *Leukemia*. 2006;20(5):833-839.
6. Lanier LL. NK cell recognition. *Annu Rev Immunol*. 2005;23:225-274.
7. Moretta A, Bottino C, Vitale M, et al. Activating receptors and coreceptors involved in human natural killer cell-mediated cytolysis. *Annu Rev Immunol*. 2001;19:197-223.
8. Cooper MA, Fehniger TA, Caligiuri MA. The biology of human natural killer-cell subsets. *Trends Immunol*. 2001;22(11):633-640.
9. Kiladjian JJ, Bourgeois E, Lobe I, et al. Cytolytic function and survival of natural killer cells are severely altered in myelodysplastic syndromes. *Leukemia*. 2006;20(3):463-470.
10. Epling-Burnette PK, Bai F, Painter JS, et al. Reduced natural killer (NK) function associated with high-risk myelodysplastic syndrome (MDS) and reduced expression of activating NK receptors. *Blood*. 2007;109(11):4816-4824.
11. Carlsten M, Baumann BC, Simonsson M, et al. Reduced DNAM-1 expression on bone marrow NK cells associated with impaired killing of CD34+ blasts in myelodysplastic syndrome. *Leukemia*. 2010;24(9):1607-1616.

12. Alderson KL, Sondel PM. Clinical cancer therapy by NK cells via antibody-dependent cell-mediated cytotoxicity. *J Biomed Biotechnol*. 2011;2011:379123.
13. Scott AM, Wolchok JD, Old LJ. Antibody therapy of cancer. *Nat Rev Cancer*. 2012;12(4):278-287.
14. Gleason MK, Verneris MR, Todhunter DA, et al. Bispecific and trispecific killer cell engagers directly activate human NK cells through CD16 signaling and induce cytotoxicity and cytokine production. *Mol Cancer Ther*. 2012;11(12):2674-2684.
15. Vallera DA, Zhang B, Gleason MK, et al. Heterodimeric Bispecific Single-Chain Variable-Fragment Antibodies Against EpCAM and CD16 Induce Effective Antibody-Dependent Cellular Cytotoxicity Against Human Carcinoma Cells. *Cancer Biother Radiopharm*. 2013.
16. Wiernik A, Foley B, Zhang B, et al. Targeting Natural Killer Cells to Acute Myeloid Leukemia In Vitro with a CD16 x 33 Bispecific Killer Cell Engager and ADAM17 Inhibition. *Clin Cancer Res*. 2013;19(14):3844-3855.
17. Reiners KS, Kessler J, Sauer M, et al. Rescue of impaired NK cell activity in hodgkin lymphoma with bispecific antibodies in vitro and in patients. *Mol Ther*. 2013;21(4):895-903.
18. Singer H, Kellner C, Lanig H, et al. Effective elimination of acute myeloid leukemic cells by recombinant bispecific antibody derivatives directed against CD33 and CD16. *J Immunother*. 2010;33(6):599-608.
19. Lechner MG, Liebertz DJ, Epstein AL. Characterization of cytokine-induced myeloid-derived suppressor cells from normal human peripheral blood mononuclear cells. *J Immunol*. 2010;185(4):2273-2284.
20. Vallera DA, Todhunter DA, Kuroki DW, Shu Y, Sicheneder A, Chen H. A bispecific recombinant immunotoxin, DT2219, targeting human CD19 and CD22 receptors in a mouse xenograft model of B-cell leukemia/lymphoma. *Clin Cancer Res*. 2005;11(10):3879-3888.
21. McCall AM, Adams GP, Amoroso AR, et al. Isolation and characterization of an anti-CD16 single-chain Fv fragment and construction of an anti-HER2/neu/anti-

CD16 bispecific scFv that triggers CD16-dependent tumor cytolysis. *Mol Immunol*. 1999;36(7):433-445.

22. Bryceson YT, March ME, Ljunggren HG, Long EO. Synergy among receptors on resting NK cells for the activation of natural cytotoxicity and cytokine secretion. *Blood*. 2006;107(1):159-166.
23. Gabrilovich DI, Nagaraj S. Myeloid-derived suppressor cells as regulators of the immune system. *Nat Rev Immunol*. 2009;9(3):162-174.
24. Chen X, Eksioglu EA, Zhou J, et al. Induction of myelodysplasia by myeloid-derived suppressor cells. *J Clin Invest*. 2013.
25. Li H, Han Y, Guo Q, Zhang M, Cao X. Cancer-expanded myeloid-derived suppressor cells induce anergy of NK cells through membrane-bound TGF-beta 1. *J Immunol*. 2009;182(1):240-249.
26. Hoechst B, Voigtlaender T, Ormandy L, et al. Myeloid derived suppressor cells inhibit natural killer cells in patients with hepatocellular carcinoma via the NKp30 receptor. *Hepatology*. 2009;50(3):799-807.
27. Kerndrup G, Meyer K, Ellegaard J, Hokland P. Natural killer (NK)-cell activity and antibody-dependent cellular cytotoxicity (ADCC) in primary preleukemic syndrome. *Leuk Res*. 1984;8(2):239-247.
28. Fauriat C, Long EO, Ljunggren HG, Bryceson YT. Regulation of human NK-cell cytokine and chemokine production by target cell recognition. *Blood*. 2010;115(11):2167-2176.
29. Ostrand-Rosenberg S, Sinha P, Beury DW, Clements VK. Cross-talk between myeloid-derived suppressor cells (MDSC), macrophages, and dendritic cells enhances tumor-induced immune suppression. *Semin Cancer Biol*. 2012;22(4):275-281.
30. Ochoa AC, Zea AH, Hernandez C, Rodriguez PC. Arginase, prostaglandins, and myeloid-derived suppressor cells in renal cell carcinoma. *Clin Cancer Res*. 2007;13(2 Pt 2):721s-726s.

31. Almand B, Clark JI, Nikitina E, et al. Increased production of immature myeloid cells in cancer patients: a mechanism of immunosuppression in cancer. *J Immunol*. 2001;166(1):678-689.
32. Diaz-Montero CM, Salem ML, Nishimura MI, Garrett-Mayer E, Cole DJ, Montero AJ. Increased circulating myeloid-derived suppressor cells correlate with clinical cancer stage, metastatic tumor burden, and doxorubicin-cyclophosphamide chemotherapy. *Cancer Immunol Immunother*. 2009;58(1):49-59.
33. Görgün GT, Whitehill G, Anderson JL, et al. Tumor-promoting immune-suppressive myeloid-derived suppressor cells in the multiple myeloma microenvironment in humans. *Blood*. 2013;121(15):2975-2987.
34. Piccioli D, Sbrana S, Melandri E, Valiante NM. Contact-dependent stimulation and inhibition of dendritic cells by natural killer cells. *J Exp Med*. 2002;195(3):335-341.
35. Terme M, Tomasello E, Maruyama K, et al. IL-4 confers NK stimulatory capacity to murine dendritic cells: a signaling pathway involving KARAP/DAP12-triggering receptor expressed on myeloid cell 2 molecules. *J Immunol*. 2004;172(10):5957-5966.
36. Vitale M, Della Chiesa M, Carlomagno S, et al. NK-dependent DC maturation is mediated by TNFalpha and IFNgamma released upon engagement of the NKp30 triggering receptor. *Blood*. 2005;106(2):566-571.
37. Gerosa F, Gobbi A, Zorzi P, et al. The reciprocal interaction of NK cells with plasmacytoid or myeloid dendritic cells profoundly affects innate resistance functions. *J Immunol*. 2005;174(2):727-734.
38. Movahedi K, Guilliams M, Van den Bossche J, et al. Identification of discrete tumor-induced myeloid-derived suppressor cell subpopulations with distinct T cell-suppressive activity. *Blood*. 2008;111(8):4233-4244.
39. Gallina G, Dolcetti L, Serafini P, et al. Tumors induce a subset of inflammatory monocytes with immunosuppressive activity on CD8+ T cells. *J Clin Invest*. 2006;116(10):2777-2790.
40. Kusmartsev S, Gabrilovich DI. STAT1 signaling regulates tumor-associated macrophage-mediated T cell deletion. *J Immunol*. 2005;174(8):4880-4891.

41. Zhao X, Rong L, Li X, et al. TNF signaling drives myeloid-derived suppressor cell accumulation. *J Clin Invest*. 2012;122(11):4094-4104.
42. Yang R, Cai Z, Zhang Y, Yutzy WH, Roby KF, Roden RB. CD80 in immune suppression by mouse ovarian carcinoma-associated Gr-1+CD11b+ myeloid cells. *Cancer Res*. 2006;66(13):6807-6815.
43. Huang B, Pan PY, Li Q, et al. Gr-1+CD115+ immature myeloid suppressor cells mediate the development of tumor-induced T regulatory cells and T-cell anergy in tumor-bearing host. *Cancer Res*. 2006;66(2):1123-1131.
44. Serafini P, Mgebroff S, Noonan K, Borrello I. Myeloid-derived suppressor cells promote cross-tolerance in B-cell lymphoma by expanding regulatory T cells. *Cancer Res*. 2008;68(13):5439-5449.
45. Zou JX, Rollison DE, Boulware D, et al. Altered naive and memory CD4+ T-cell homeostasis and immunosenescence characterize younger patients with myelodysplastic syndrome. *Leukemia*. 2009;23(7):1288-1296.
46. Kordasti SY, Ingram W, Hayden J, et al. CD4+CD25high Foxp3+ regulatory T cells in myelodysplastic syndrome (MDS). *Blood*. 2007;110(3):847-850.
47. Kotsianidis I, Bouchliou I, Nakou E, et al. Kinetics, function and bone marrow trafficking of CD4+CD25+FOXP3+ regulatory T cells in myelodysplastic syndromes (MDS). *Leukemia*. 2009;23(3):510-518.
48. Hanson EM, Clements VK, Sinha P, Ilkovitch D, Ostrand-Rosenberg S. Myeloid-derived suppressor cells down-regulate L-selectin expression on CD4+ and CD8+ T cells. *J Immunol*. 2009;183(2):937-944.
49. Romee R, Foley B, Lenvik T, et al. NK cell CD16 surface expression and function is regulated by a disintegrin and metalloprotease-17 (ADAM17). *Blood*. 2013;121(18):3599-3608.
50. Rabinovich GA, Gabrilovich D, Sotomayor EM. Immunosuppressive strategies that are mediated by tumor cells. *Annu Rev Immunol*. 2007;25:267-296.
51. Klinger M, Brandl C, Zugmaier G, et al. Immunopharmacologic response of patients with B-lineage acute lymphoblastic leukemia to continuous infusion of T cell-

engaging CD19/CD3-bispecific BiTE antibody blinatumomab. *Blood*. 2012;119(26):6226-6233.

52. Topp MS, Kufer P, Gökbuget N, et al. Targeted therapy with the T-cell-engaging antibody blinatumomab of chemotherapy-refractory minimal residual disease in B-lineage acute lymphoblastic leukemia patients results in high response rate and prolonged leukemia-free survival. *J Clin Oncol*. 2011;29(18):2493-2498.
53. Topp MS, Gökbuget N, Zugmaier G, et al. Long-term follow-up of hematologic relapse-free survival in a phase 2 study of blinatumomab in patients with MRD in B-lineage ALL. *Blood*. 2012;120(26):5185-5187.

## APPENDIX

## Appendix Table 1: Demographics of the MDS Patient Cohort

| Variables | No. of Patients (%) |
|---|---|
| | |
| ***Sex*** | |
| Male | 40 (60%) |
| Female | 27 (40%) |
| | |
| [a]Age (years) | 47 (19-74) |
| | |
| ***Ethnicity*** | |
| Caucasian | 62 (93%) |
| African-American | 2 (3%) |
| Hispanic | 2 (3%) |
| Other | 1 (1%) |
| | |
| ***FAB Subtype*** | |
| RAEB-T | 10 (15%) |
| RAEB | 24 (36%) |
| RARS | 8 (12%) |
| RA | 9 (13%) |
| [b]Other | 16 (24%) |
| | |
| [c]***Karyotype (IPSS)*** | |
| Favorable | 24 (36%) |
| Intermediate | 9 (14%) |
| Poor | 15 (22%) |
| Unknown | 19 (28%) |
| | |
| [d]***Blast Percentage (IPSS)*** | |
| <5% | 35 (52%) |
| 5 - 10% | 14 (21%) |
| 11 - 20% | 3 (4%) |
| ≥21% | 5 (8%) |
| Unknown | 10 (15%) |
| | |
| [e]***MDS Status*** | |
| Lower Risk | 24 (36%) |
| Higher Risk | 41 (61%) |
| Unknown | 2 (3%) |

Abbreviations: FAB: French-American-British classification; RAEB-T: Refractory anemia with excess blasts in transformation; RAEB: Refractory anemia with excess blasts; RARS: Refractory anemia with ringed sideroblasts; RA: Refractory anemia; IPSS: International prognosis scoring system.

[a]Median (range) age at date of transplant

[b]Other: Paroxysmal nocturnal hemoglobinuria; Polycythemia vera; Essential thrombocythemia; Myelofibrosis with myeloid metaplasia; Myelofibrosis or myelosclerosis; Myelodysplasia or myloproliferative disorder.

[c]Favorable: normal karyotype, isolated –Y, del(5q) or del(20q); Intermediate: other abnormalities; Poor: complex (≥3 abnormalities) or chromosome 7 anomalies.

[d]Blast percentage at date of transplant

[e]Lower Risk: RA or RARS; Higher Risk: RAEB, RAEB-T or CMML. Data regarding specific cell counts were not available, thus we were unable to determine the overall IPSS scores

**Appendix Table 2: MDS cell population frequencies and CD16xCD33 BiKE-induced MDS NK cell function stratified by blast percentage (IPSS)**

| | [a]*Blast Percentage (IPSS)* | | | | |
|---|---|---|---|---|---|
| | <5% (n=35) | 5-10% (n=14) | 11-20% (n=3) | ≥21% (n=5) | Unknown (n=10) |
| % NK cells | 2 ± 0.3% | 3 ± 1% | 0.2 ± 0.1% | 2 ± 1% | 1 ± 0.3% |
| % $CD33^+$ | 28 ± 3% | 29 ± 6% | 56 ± 12% | 23 ± 7% | 28 ± 7% |
| % MDSC | 21 ± 3% | 23 ± 4% | 38 ± 9% | 20 ± 6% | 14 ± 3% |
| | | | | | |
| [b]**PBMC Alone** | | | | | |
| % $CD107a^+$ | 38 ± 3% | 33 ± 5% | 33 ± 18% | 30 ± 6% | 42 ± 4% |
| % TNF-$\alpha^+$ | 4 ± 1% | 5 ± 2% | 5 ± 4% | 6 ± 4% | 4 ± 1% |
| % IFN-$\gamma^+$ | 5 ± 1% | 3 ± 0.4% | 7 ± 3% | 4 ± 1% | 2 ± 1% |
| | | | | | |
| [c]**PBMC + HL-60** | | | | | |
| % $CD107a^+$ | 42 ± 2% | 42 ± 4% | 34 ± 17% | 46 ± 3% | 45 ± 4% |
| % TNF-$\alpha^+$ | 11 ± 2% | 12 ± 2% | 13 ± 8% | 17 ± 4% | 16 ± 2% |
| % IFN-$\gamma^+$ | 14 ± 2% | 13 ± 2% | 9 ± 5% | 23 ± 6% | 18 ± 3% |

[a]Blast percentage at date of transplant
[b]CD16xCD33 BiKE induced MDS-NK cell function in the absence of HL-60 targets
[c]CD16xCD33 BiKE induced MDS-NK cell function in the presence of HL-60 targets

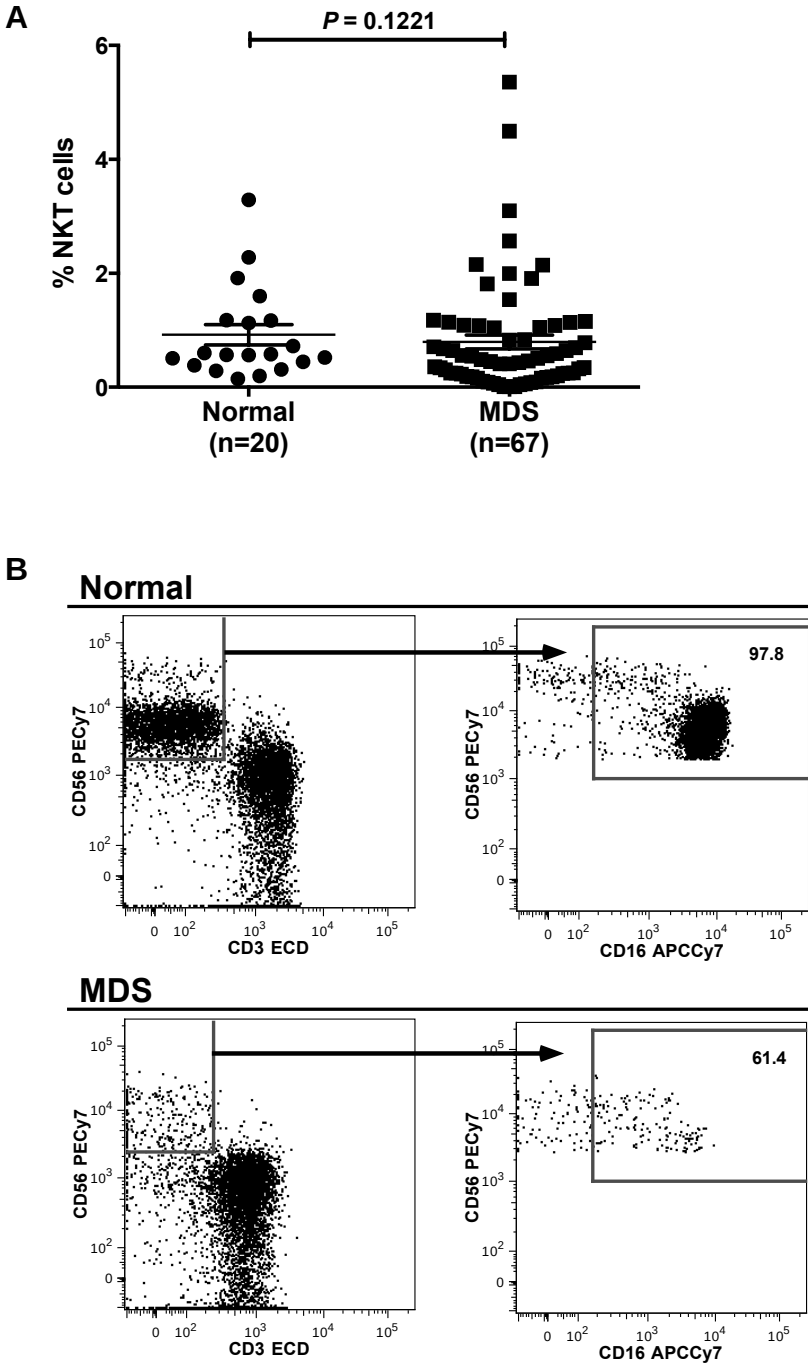


**Appendix Figure 1: NKT cell frequency and NK cell CD16 expression among MDS patients.**

(A) Percent of $CD56^+/CD3^+$ NKT cells (normalized to all cell fraction based on the FSC/SSC gate excluding debris). (B) Normal donor and MDS-NK cells were stained with anti-CD45, anti-CD7, anti-CD56, anti-CD3 and anti-CD16 mAb and analyzed by flow cytometry. Representative flow cytometry plots from one normal donor (#14) and one higher risk MDS patient (#31) of percent of $CD16^+$ NK cells are shown.

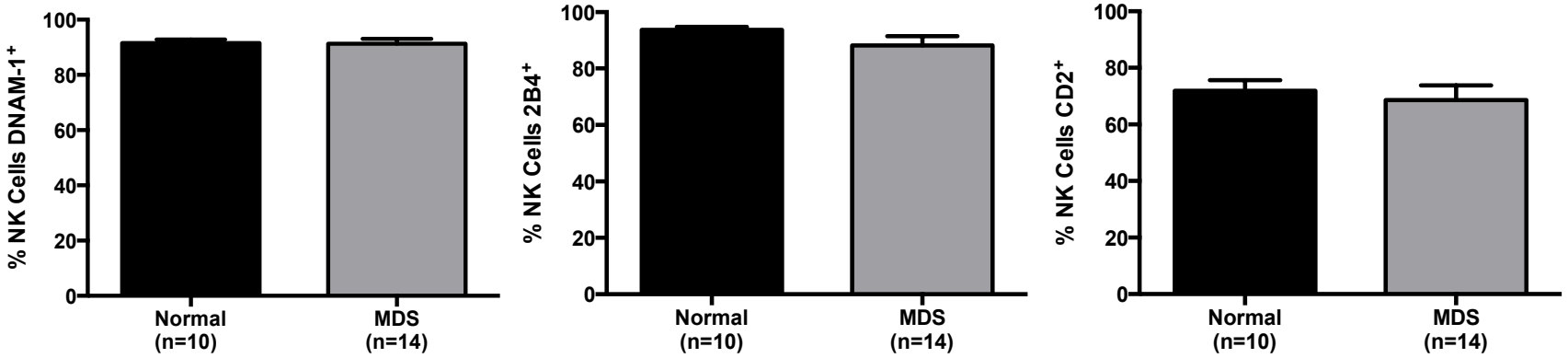


**Appendix Figure 2: DNAM-1, 2B4 and CD2 MDS-NK cell receptor expression.**
Normal donor and MDS-NK cells were stained with anti-CD45, anti-CD7, anti-CD56, anti-CD3, anti-DNAM-1, anti-2B4 and anti-CD2 mAb and surface receptor expression of DNAM-1, 2B4 and CD2 on NK cells were evaluated by flow cytometry.

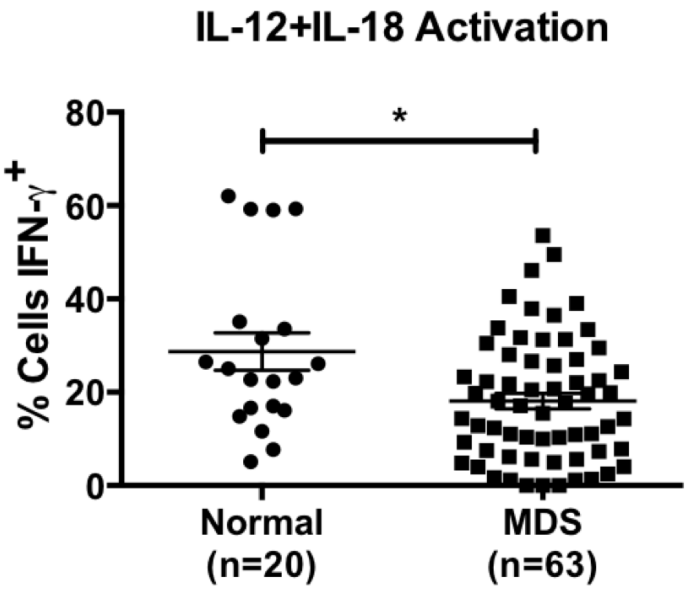


**Appendix Figure 3: IFN-γ production of MDS-NK cells is lower compared to normal donors after IL-12 and IL-18 activation.**
PBMC from normal donors and MDS patients were stimulated overnight with IL-12 (10ng/mL) and IL-18 (100ng/mL) and NK cell intracellular IFN-γ production was evaluated via FACS analysis (**P*<0.05).

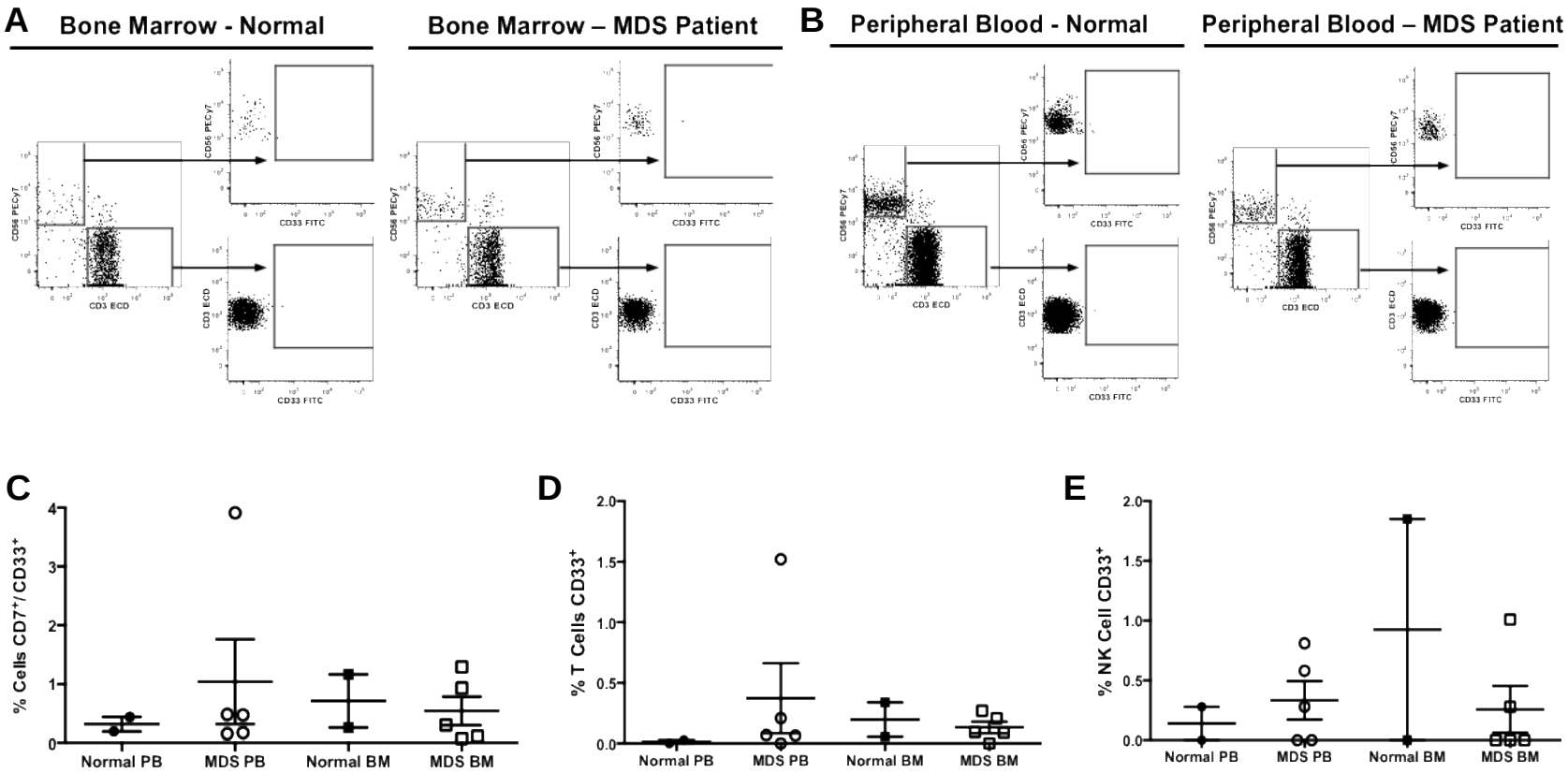


**Appendix Figure 4: CD33 Expression on lymphocyte populations**.
Bone marrow (BM) and peripheral blood (PB) from normal donors and MDS patients were stained with anti-CD45, anti-CD7, anti-CD56, anti-CD3 and anti-CD33 and CD33 expression was evaluated by flow cytometry on $CD7^+$, T and NK cell populations. Flow cytometry plots are representative of one normal donor and one MDS patient and show CD33 expression on (A) $CD56^-/CD3^+$ T cells and (B) $CD56^+/CD3^-$ NK cells. Aggregate data for CD33 expression on (C) $CD7^+$ lymphocytes, (D) T cells and (E) NK cells from normal donors (n=2) and MDS patients (n=5) from BM and PB are shown.

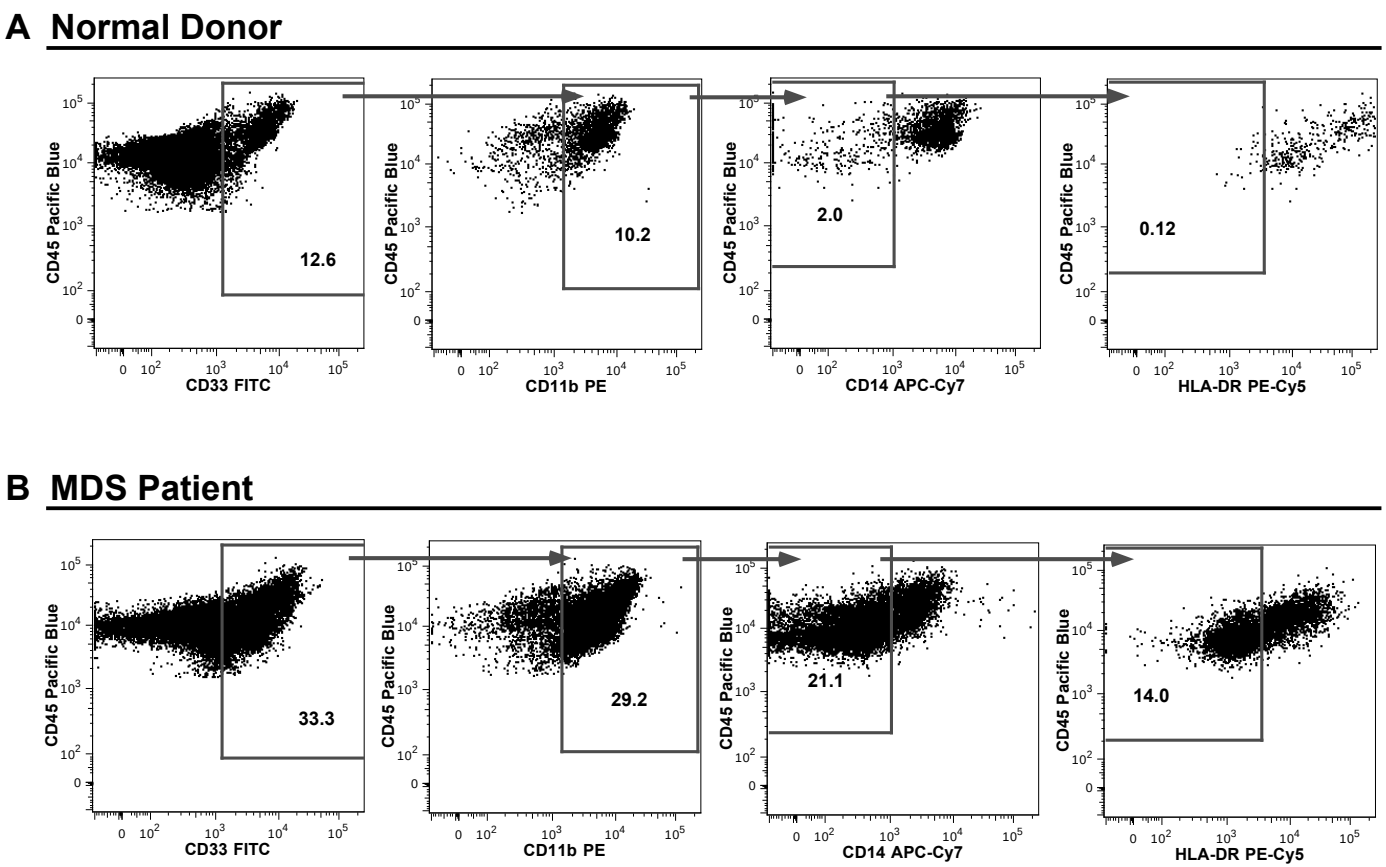


**Appendix Figure 5: MDSC gating strategy.**
PBMC from normal donors and MDS patients were stained with anti-CD45, anti-CD33, anti-CD11B, anti-CD14 and anti-HLA-DR mAbs. (A-B) Gating strategy for the evaluation of MDSC population in normal donors (A) and MDS patients (B). Plots are representative from one normal donor (#3 of 20) and one higher risk MDS patient (#25 of 67) and gate frequency indicates population percent normalized to the all cell fraction based on the FSC/SSC gate excluding debris.

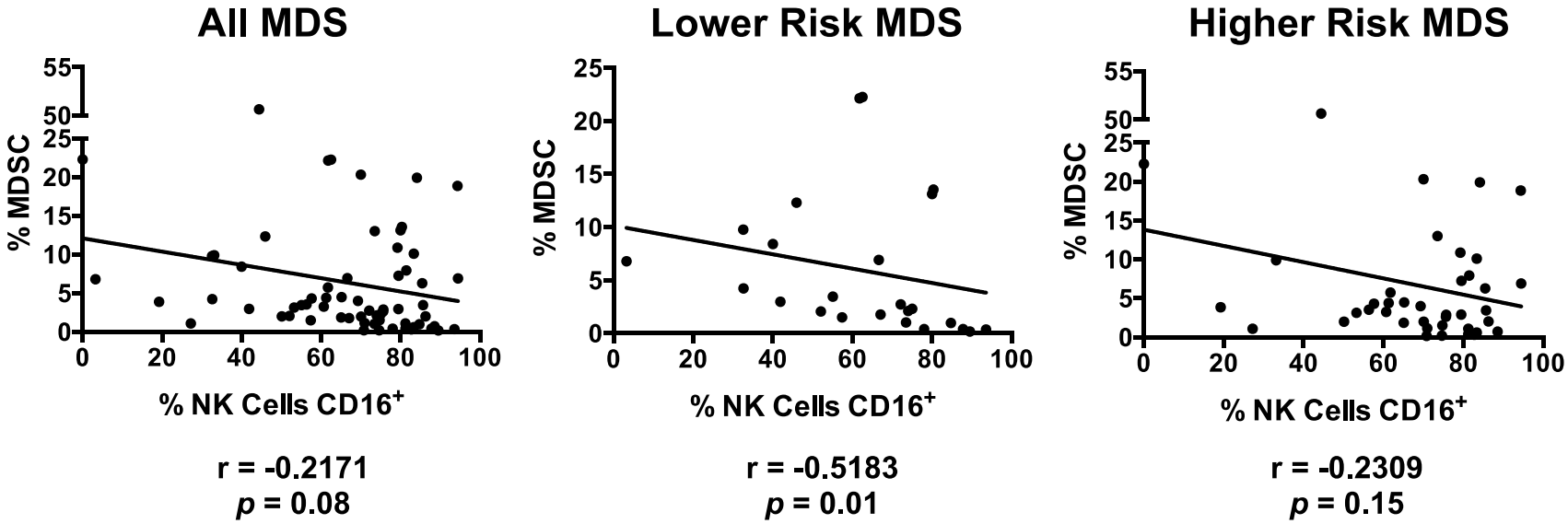


**Appendix Figure 6: MDS-NK cell CD16 expression negatively correlates with MDS-MDSC frequency.**
PBMC from MDS patients were stained with anti-CD45, anti-CD7, anti-CD56, anti-CD3, anti-CD16, anti-CD33, anti-CD11b, anti-CD14 and anti-HLA-DR mAbs. The correlations between % MDSC (normalized to all cell fraction excluding debris) and % NK cells $CD16^+$ among all MDS patients, lower risk MDS patients and higher risk MDS patients are presented. Correlation coefficients (r) and statistical significance are indicated in the figure.

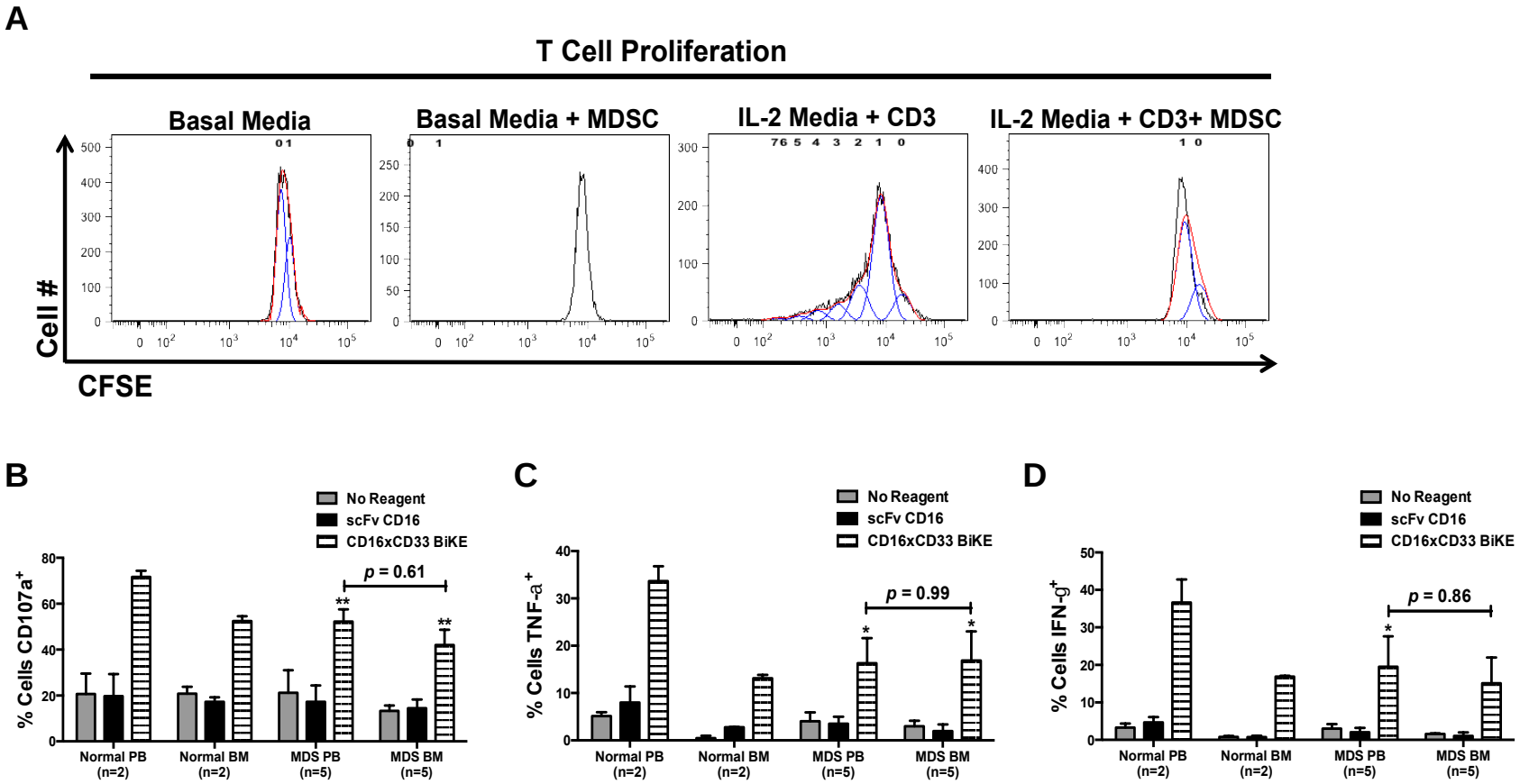


**Supplemental Figure 7: CD16xCD33 BiKE enhances peripheral blood and bone marrow NK cell function against HL-60 targets**.
(A) CFSE-labeled T cells were cultured for 5 days in basal medium, medium supplemented with 100U/mL IL-2 and CD3 bead activation in the presence or absence (E:T ratio = 1:2) of cytokine-derived MDSC from normal PBMC and proliferation was evaluated via FACS analysis. Histogram plots represent one of six normal donors. (B-D) Mononuclear cells from peripheral blood (PB) and bone marrow (BM) were isolated from normal donors (n=2) and MDS patients (n=5), coated with 10μg/mL of CD16xCD33 BiKE or scFv CD16 control, co-cultured with HL-60 targets and NK cell (B) CD107a expression and intracellular (C) TNF-α and (D) IFN-γ production were evaluated via FACS analysis (*$P$<0.05, **$P$<0.01).

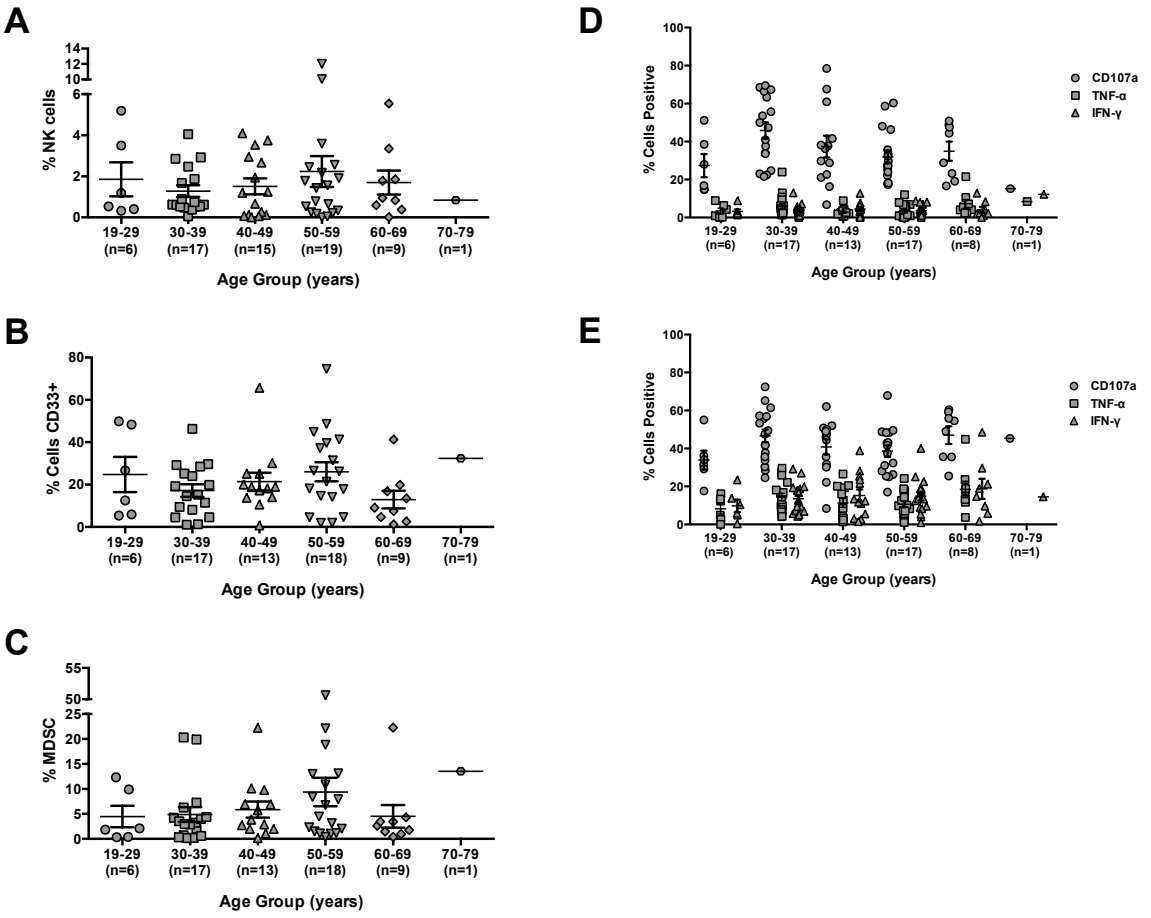


**Appendix Figure 8: CD16xCD33 BiKE consistently enhances MDS-NK cell function among all age strata**.

The percent of $CD56^+/CD3^-$ MDS-NK cells (A), total $CD33^+$ cells (B) and MDS-MDSC (C) of the all cell fraction was stratified according to age groups (years). (D-E) CD16xCD33 BiKE-induced MDS-NK cell functions (degranulation (CD107a), intracellular TNF-α and IFN-γ production) in the absence of HL-60 targets (D) and in the presence of HL-60 targets (E) were stratified according to age groups. Y-axis of graphs (D and E) represent the percent of NK cells positive for each function listed in graph legend.